In vitro behavior of sintered compacts of Co-Cr doped with hydroxyapatite for biomedical implants

D.I. BĂILĂ[a], O.C. MOCIOIU[b], C. ZAHARIA[a], R. TRUŞCĂ[c], A. SURDU[a], M. BUNEA[a]
[a]*University POLITEHNICA of Bucharest, 313 Splaiul Independentei, district 6, 060042, Bucharest, Romania;*
[b]*"Ilie Murgulescu" Institute of Physical Chemistry of the Romanian Academy, 202 Splaiul Independentei, district 6, 060021, Bucharest, Romania;*
[c]*METAV, 313 Splaiul Independentei, district 6, 060042, Bucharest, Romania;*

The purpose of this study was to obtain Co-Cr sintered compacts doped with hydroxyapatite (HA) in order to improve the bioactivity of implants and the in vitro behavior after an immersion in simulated biological fluid (SBF 1x) for 7 days. Co-Cr powder (ST2724G) was used to realize four compacts doped with 5wt% HA, 10wt% HA, 15wt% HA and 20wt%HA. The comparison is realized using a Co-Cr blind sample. Scanning electronic microscopy (SEM) coupled with x-ray spectrometer for energy dispersive (EDS) and x-ray diffraction analysis (XRD) were employed for semiquantitative and qualitative chemical and metallographic analyses. After immersion in SBF for 7 days can be noticed the growth of hydroxyapatite on the surface of all compacts doped with HA. The bioactivity resulted from immersion in SBF for 7 days of Co-Cr compacts has been improved by doping with hydroxyapatite.

(Received May 27, 2015; accepted June 24, 2015)

Keywords: Biocompatibility, Hydroxyapatite, In vitro test

1. Introduction

Human bone consists of cylindrical chanels, osteons that are held together by a framework of hard tissue, mainly natural hydroxyapatite [1,2]. Osteons, the major organic component of bone fill the pores of 190-230 μm size of bones. The inorganic matrix of bone consists of a porous structure. For bone ingrowth to occur into a porous ceramic bone, substitute material, the natural bone structure, the typical pore size must be greater that 100 μm.

For an implant it is important that only the parts that are in contact with the bone must present a hydroxyapatite phase, like bioactive phase with osteoconductive importance. The presence of bioactive phase allow the formation of new calcium phosphates [3-12].

The most used metalic materials for bone implants manufacturing are Ti6Al4V [13], Ti-Ni alloys [14-16], stainless steel 304 or 316L [17-19], and Co-Cr alloys [20].

The powder of Co-Cr alloy presents good mechanical strength, good resistance to corrosion and a degree of cleaning identical to that of the glass [21-23]. The author has been done similar research on the sintered compacts of the Ti6Al4V alloy powder doped with different percentages of hydroxyapatite and sintered at 700^{o}C [11, 12, 23]. The amount 10 wt% HA for doping of Ti6Al4V sintered compacts were found to be optimal for implants and with a good mechanical strength [23]. Powder of Co-Cr alloy is considered tolerable in dentistry domain and is used for the realization of dental crowns, bridges and chapels.

The Co-Cr powders can be used for direct metal laser sintering (DMLS) process because they have good sintering properties and the size and the spherical form of grain permit to obtain sintering samples [24]. Direct metal laser sintering is a rapid prototyping technique and uses a laser as the power source and sintered the metallic powder material, aiming the laser automatically at points in space defined by a 3D model, binding the material together to create a solid structure.

The grains of Co-Cr powder are ranging around 20 microns size. [25-32] The low size distribution of alloy powder allows a better control of the thermal gradient during the contact between the material and the laser, providing the following advantages: an excellent material quality and surface status; limited mechanical stress within the part being produced; increased definition of the details; reduction in size of production supports.

In the contact zone of the implant with bone, the presence of phosphates of calcium favors the mineral kernel on bone. [33, 34]

The aim of our work was to obtain Co-Cr sintered compacts doped with hydroxyapatite for improvement of implants bioactivity.

2. Experimental

In this work were obtained dental implants materials with bioactive behavior in bone tissue, using Co-Cr powders (ST2724G) used for direct metal laser sintering (DMLS) process and hydroxyapatite powders. Chemical composition of Co-Cr alloy is 54.31 %Co; 23.08%Cr; 7.85% W, 3.35% Si and Mn, Fe <0.1. In the table 1 are presented main mechanical properties of Co-Cr alloy powder used in preparation of compacts.

Commercial hydroxyapatite $Ca_3(PO_4)_2$ powder (Sigma Aldrich) with a purity p.a greater that 90% was used for

doping. In the Fig. 1 the SEM result show acicular morphology of the hydroxyapatite powder and the grain size of 10-100 nm. The commercial hydroxyapatite (HA) was characterized by EDS and XRD shown in Fig. 2 and Figure 3. In the contact zone of the implant with bone, the presence of phosphates of calcium favors the mineral kernel on bone.

Table 1. Mechanical properties of Co-Cr alloy powder

Engineering Property	Values
Elastic limit 0,2% (Rp0,2)	815 MPa
Elongation at break	10%
Vickers hardness	375 HV 5
Elastic module	229 GPa
Volume mass	8,336 $g.cm^{-3}$
Corrosion resistance	< 4µg/cm^2
Thermal expansion coefficient	14,5 10^{-6} K^{-1}

The Co-Cr sintered compacts doped with hydroxyapatite were realized for the study of the bioactivity in simulated biological fluid SBF for 7 days. Different compacts were realized starting from powder Co-Cr and 5%, 10%, 15%, 20% hydroxyapatite (percentage by mass).

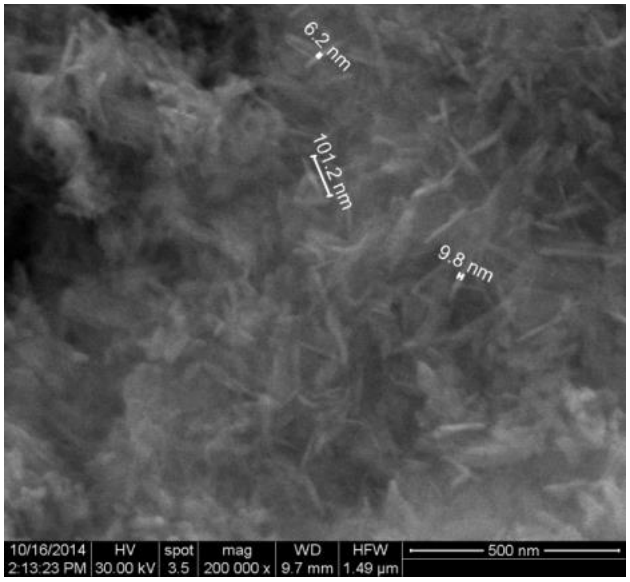

Fig. 1. SEM image of hydroxyapatite (X 200 000)

A blind sample was realized from Co-Cr alloy powder. The raw materials were homogenized 30 minutes, and the ethanol was used. The samples powders were pressed into the mould to active section of 1 cm^2, without the introduction of lubricant. The compacts were realized using a pressure of 20 Kg/cm^2. The samples were sintered in an electrical furnace after a complex regime multistage. In first stage of sintering the samples were heated with a heating rate of 2°/minute to 250^{0}C where a plateau of 10 minutes was maintained in order to remove water and organic residues; followed by the second stage of sintering at 700°C for 30 minutes, using a heating rate of 10°/minute. The cooling of sintered compacts was conducted slowly, up to ambient temperature.

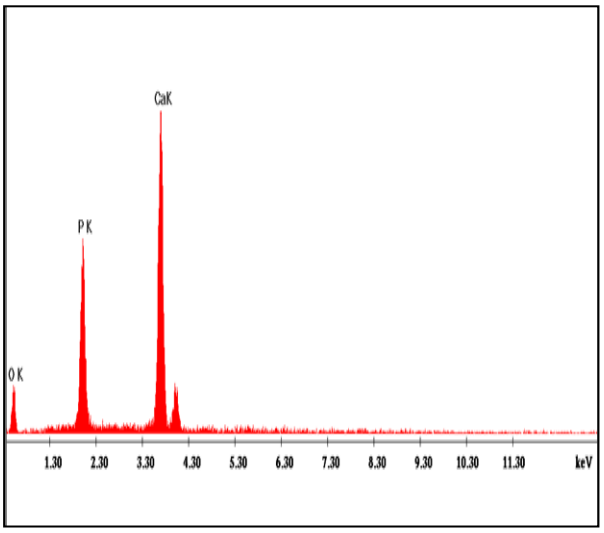

Fig. 2. EDS of hydroxyapatite

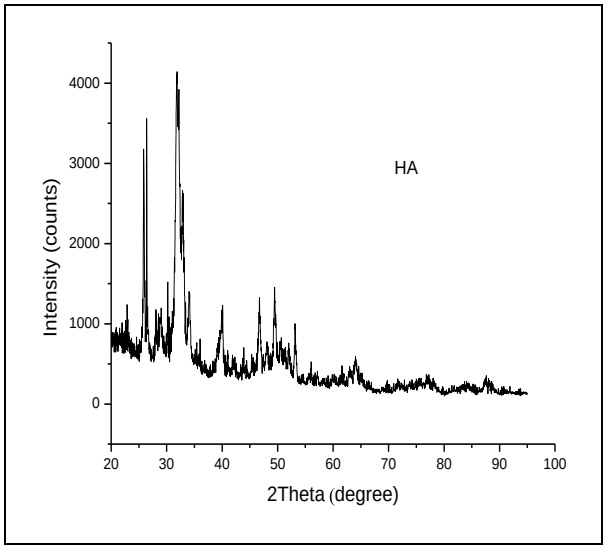

Fig. 3. XRD pattern of hydroxyapatite

SEM, EDS and XRD analysis investigated the sintered compacts. The bioactivity was evidenced by immersion in SBF for 7 days. In this period, the SBF has greened for all compacts this demonstrates that reaction between compacts and SBF occurs with joining of several molecules of hydroxyapatite to the Co-Cr compacts.

Investigation of morphology and semi-quantitative analysis of samples were performed using scanning electron microscope QUANTA INSPECT F equipped with

electron gun with field emission -FEG (field emission gun) with a resolution of 1.2 nm and x-ray spectrometer for energy dispersive (EDS) with a resolution of 133eV at MnK. For the chemical composition of the samples studied were used out images of secondary electrons and backscatter electron images, the bright contrast micro areas contain heavy elements (no. Atomic large) and the dark contrast of light elements are employed. The areas of interest were analysed qualitatively by micro compositional X-ray spectrometry.

XRD analysis was performed using an X-ray diffractometer that uses PAnalytical Empyrial characteristic CuKα radiation and wavelength 1.541874. Spectrum acquisition was performed in Bragg-Brentano geometry.

For mineralization assay, three samples of each material were incubated in synthetic body fluid (SBF1x) at pH=7.4, adjusted with tris(hydroxy-methyl) aminomethane (Tris) and hydrochloric acid (HCl), for 7 days, under sterile conditions, in containers with 45 mL of the incubation medium at 37ºC. The incubation medium was changed every 48 h. After incubation, the specimens were rinsed with distilled water to remove any traces of salts from the surface and dried at 40 ºC for 24 h.

The composition of SBF1x is presented below: 142.19 mM (Na^+); 2.49 mM (Ca^{2+}); 1.5 mM (Mg^{2+}); 4.2 mM (HCO_3^-); 141.54 mM (Cl^-); 0.9 mM (HPO_4^{2-}); 0.5 mM (SO_4^{2-}); 4.85 mM (K^+).

3. Results and discussion

In the Fig. 4 are presented the Co- Cr sintered compacts doped with hydroxyapatite.

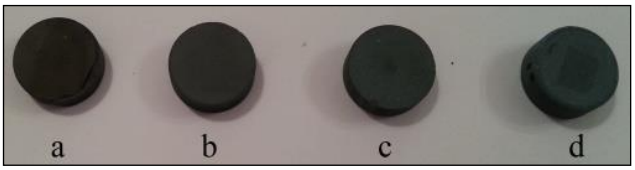

Fig. 4. Sintered compacts of Co-Cr doped with a) 5%HA b) 10%HA, c) 15%HA, d) 20%HA

3.1 Blind Co-Cr sintered compact

Blind Co-Cr sintered compact (Fig. 5) was sintered in the same condition like the Co-Cr sintered compacts doped with HA. Figure 6 present EDS analysis of blind Co-Cr sintered compact and Fig. 7 shows the XRD pattern for Co-Cr sintered compact.

The Co-Cr powder has a fine granulation with grain size around 20 μm and spherical grains morphology. In the SEM images the great particles represent Co grains and the smaller particles represent Cr grains. EDS analyse remark the presence of Co and Cr as majority mass and another elements like Si, Mn, Fe, W as traces.

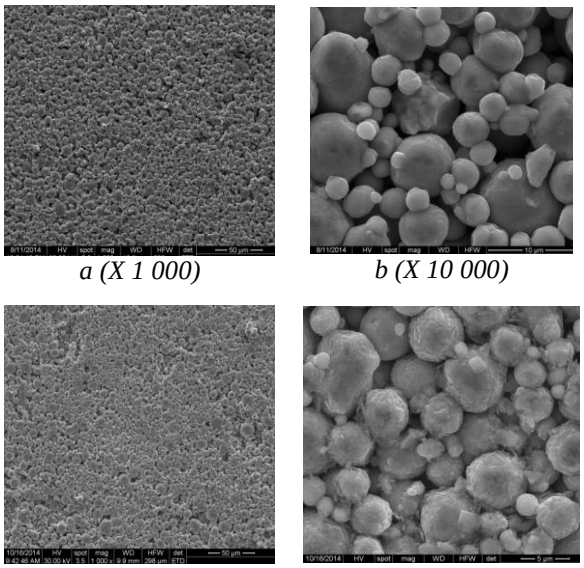

Fig. 5. SEM images of Co-Cr blind sample: a,b) initially; c,d) after immersion in SBF for 7 days.

The chemical composition was determinate by XRD and the result evidenced the chromium cobalt molybdenum with chemical formula $Cr_{0.32}Mo_{0.04}Co_{0.64}$ according with ASTM 04-016-6870.

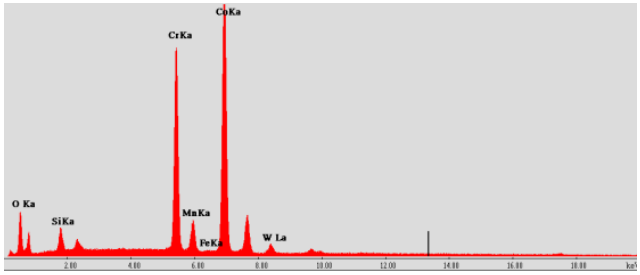

a

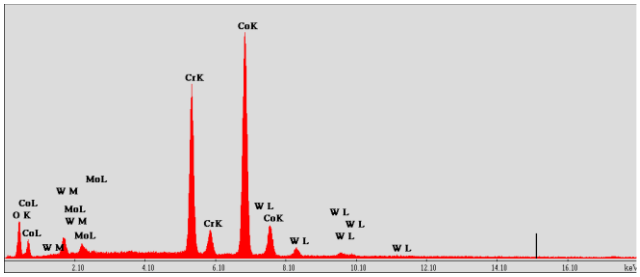

b

Fig. 6. EDS analyses of Co-Cr blind sample: a) Initially; b) After immersion in SBF for 7 days

In the case of the blind sintered compact of Co-Cr immersed in SBF for 7 days, a change occurs, a deterioration of particles as can be seen in the Figure 5.

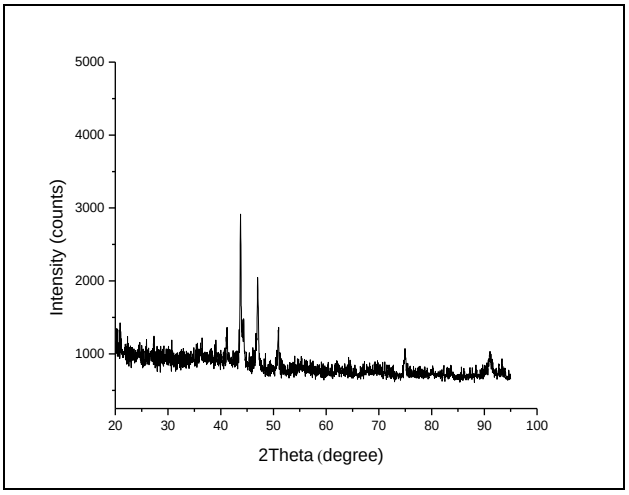

Fig. 7. XRD of Co-Cr blind sample

In EDS analysis (Fig. 6b) one can see the bright contrast areas (heavy elements with high atomic number) containing W, Cr, Co and Fe. After 7 days of immersion in SBF, XRD pattern do not present modifications concerning the chemical composition of the blind sintered compact of Co-Cr, like in Fig. 7.

3.2 Co-Cr compact sintered doped with 5%HA

In the Fig. 8 are presented SEM images of Co-Cr sintered compact doped with 5% wt HA at different magnifications.

In the Fig. 8.c. are presented measurements of grains.

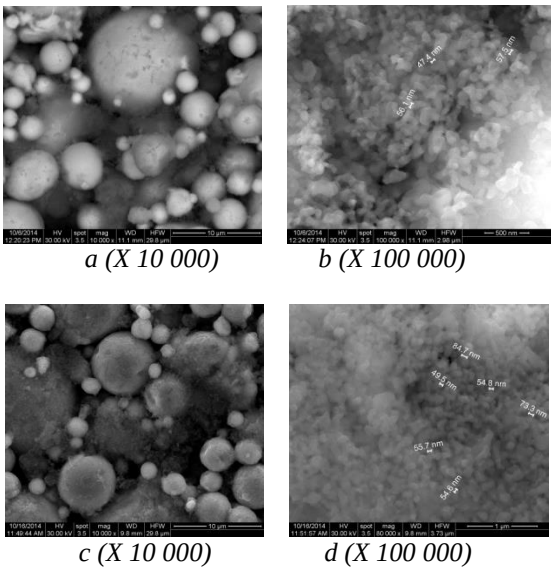

a (X 10 000) *b (X 100 000)*

c (X 10 000) *d (X 100 000)*

Fig. 8. SEM images of Co-Cr sintered compact doped with 5%HA: a,b) initially; c,d) after immersion in SBF for 7 days

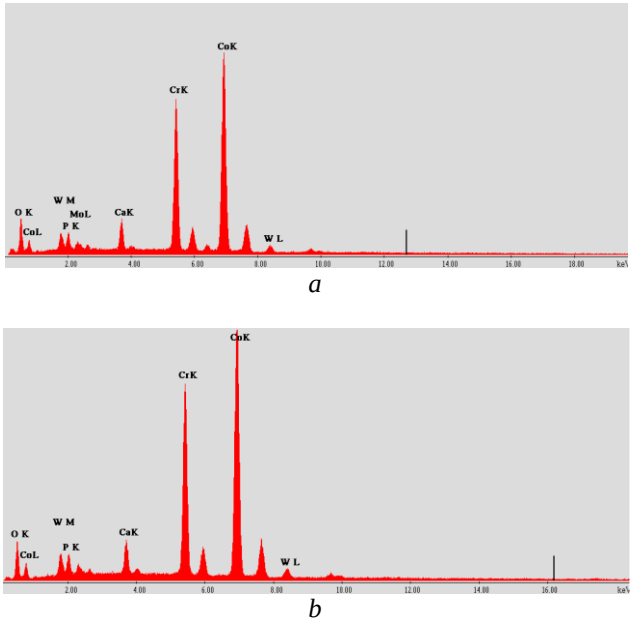

a

b

Fig. 9. EDS analyses of Co-Cr sintered compact doped with 5%HA: a) initially; b) after immersion in SBF for 7 days

Concerning to Co-Cr sintered compact with 5% HA it remarks white grains representing Co and Cr and grey grains of HA.

The larger spherical represent the grains of Co, and the smaller spherical represent the grains of Cr.

The compact present remarkable homogeneity between Co-Cr alloy and HA, as can be observed in the Figs. 8 and 9. Hydroxyapatite grains show a change of shape.

The irregular and elongated grains with nanometer size under 100μm were obtained in the compact because of sintering treatment at 700ºC. XRD patterns (figure 10) shows a mixture of peaks of HA and Co-Cr alloy.

In the case of the sintered compact Co-Cr doped with 5%HA immersed in SBF has appear aglomeration of hydroxyapatite, like in Figures 8d-8f.

EDS and XRD analyses present a little bit more hydroxyapatite after immersion in SBF.

New grains of hydroxyapatite were grown on the surface of compact after immersion in SBF for 7 days. Their dimensions are among 49-85 nm.

The grains below 57 nm can be seen in the initially compact and the grains of 70-85 nm are grown after immersion in SBF for 7 days.

The EDS results are not very different after immersion in SBF for 7 days.

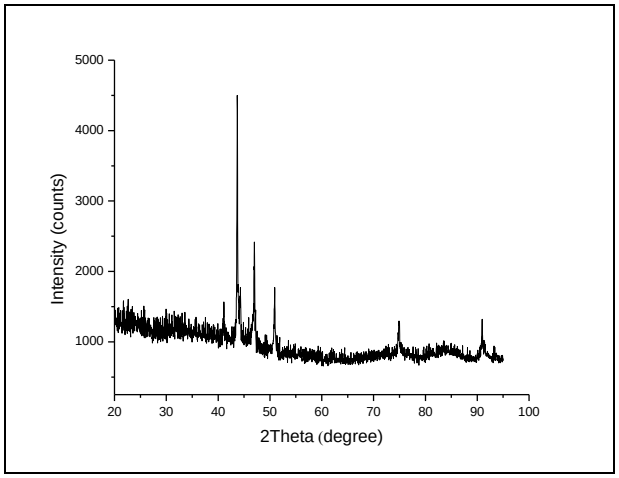

a

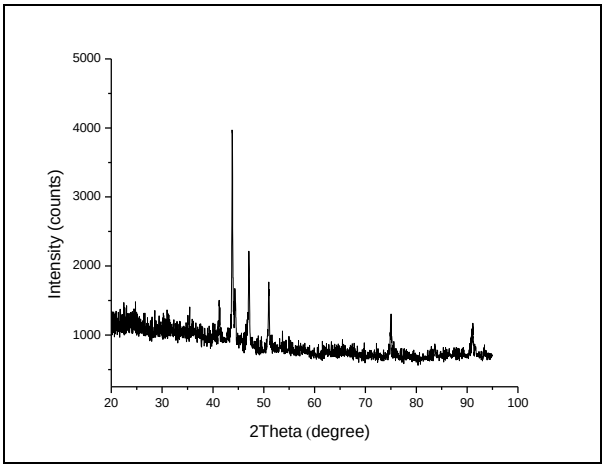

b

Fig. 10. XRD patterns of Co-Cr sintered compact doped with 5% HA: a) initially; b) after immersion in SBF for 7 days

In the maping can see bright contrast areas (heavy elements with high atomic number) containing W, Cr, Co and Fe and grey contrast areas containing Ca. XRD results show very weak peaks of HA due to small quantity added in compact.

3.3 Co-Cr compact sintered doped with 10%HA

For Co-Cr sintered compact doped with 10% HA, remark a growth concentration of HA grain, the zone grey compared to the grains of Co and Cr with white. In general figure Fig. 11(x1000) is remarkable the homogeneity of mixing Co-Cr with 10% HA. Hydroxyapatite has irregular and elongated grains with nanometer size. XRD analysis revealed the presence of HA in a concentration of 10% (fig.13a).

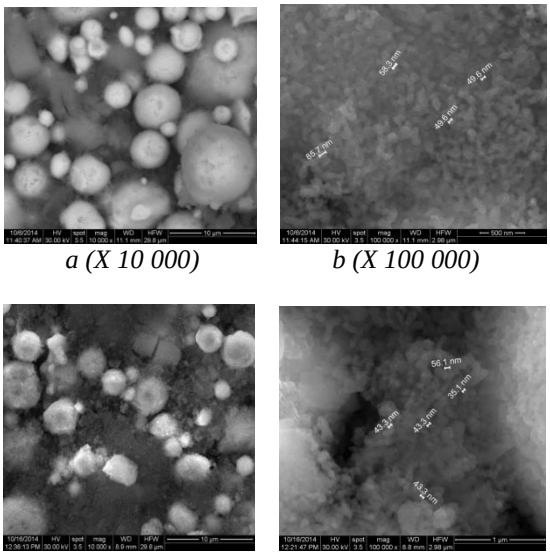

a (X 10 000) *b (X 100 000)*

c (X 10 000) *d (X 100 000)*

Fig. 11. SEM images of Co-Cr sintered compact doped with 10% HA: a,b) initially; c,d) after immersion in SBF for 7 days

After imerssion in SBF during 7 days, for the sintered compact Co-Cr doped with 10%HA remark a growth quantity of HA. Determine that the Co-Cr grains are covered with hydroxyapatite, like in Fig. 11d-f. The hydroxyapatite presents two type of grains, fines grains and incresed grains.

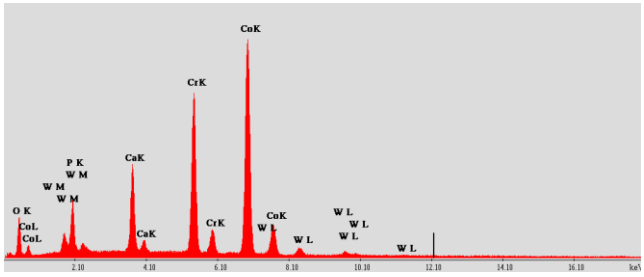

a

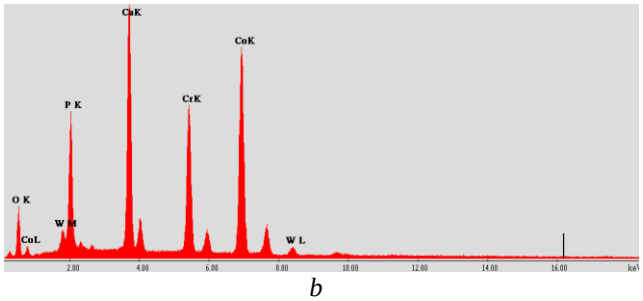

b

Fig. 12. EDS analyses of Co-Cr sintered compact doped with 10%HA: a) initially; b) after immersion in SBF for 7 days

One can observe different zones with hydroxyapatite aglomerations, because of the new hydroxyapatite grains obtains after imerssion in SBF. EDS and XRD analyses determine the quantity of hydroxyapatite and the growth concentration of HA after immersion in SBF. Can see bright contrast areas (heavy elements with high atomic number) containing W, Cr, Co and Fe and contrast grey areas containing Ca, using EDS analysis.

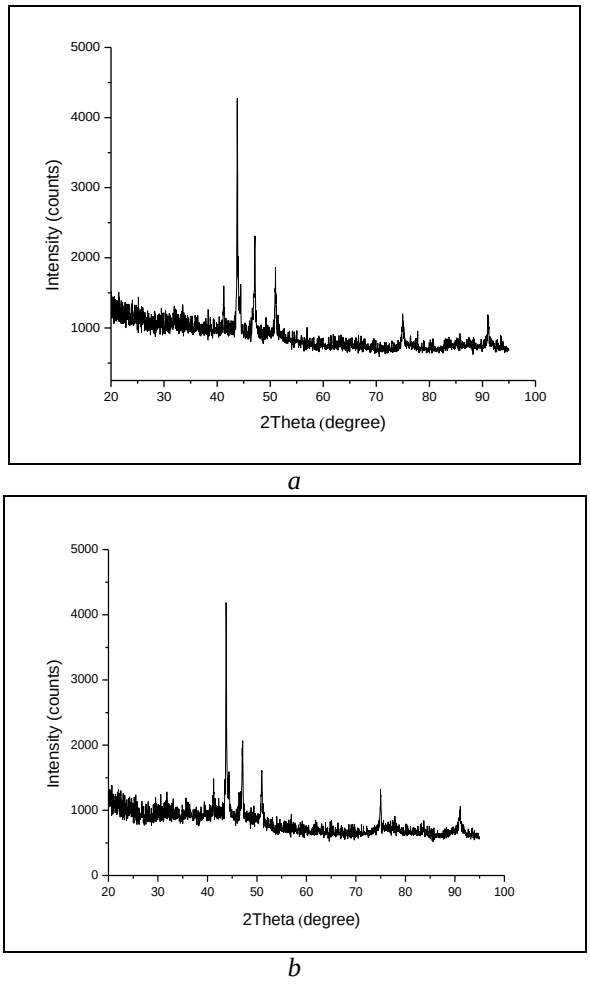

Fig. 13. XRD patterns of Co-Cr sintered compact doped with 10% HA: a) initially; b) after immersion in SBF for 7 days

XRD analyse, presents the presence of HA peaks and appear modifications concerning the chemical composition of the sintered compact of Co-Cr with 10%HA, Fig.13b). The peaks of calcium phosphate hydroxide $Ca_5(PO_4)_3(OH)$ are determinated by XRD analyses that has hexagonal crystal system.

3.4 Co-Cr compact sintered doped with 15%HA

Concerning the Co-Cr sintered compact with 15% HA also notice the growth grey zone of HA and with white the grains of Co and Cr.

In Figure14 is shown SEM images of compacts surface with a good homogeneity. Hydroxyapatite has irregular and elongated grains with nanometer size. XRD analysis revealed the presence of HA increase in concentration of 15%. The peaks determinate by XRD analysis are for calcium phosphate hydroxide $Ca_5(PO_4)_3(OH)$ with hexagonal crystal system, P63/m space group, 176 space group number. For the sintered compact Co-Cr doped with 15%HA, after immersion in SBF during 7 days, remark a growth quantity of HA.

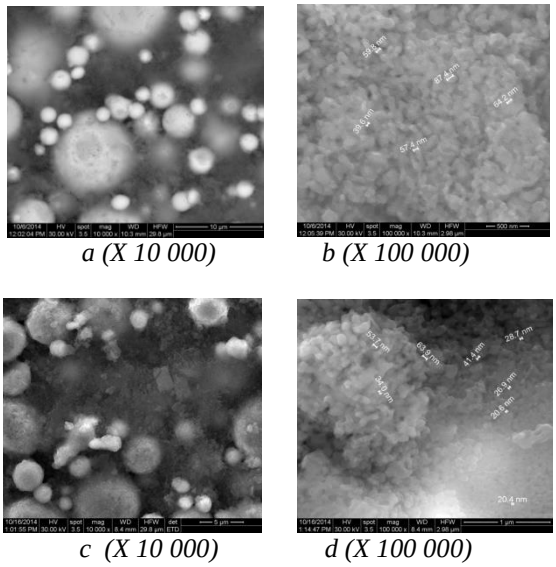

Fig. 14. SEM images of Co-Cr sintered compact doped with 15%HA: a,b) initially; c,d) after immersion in SBF for 7 days

The Co-Cr grains are cover with a generous layer of hydroxyapatite, like in Fig.14d-f. Remark two generation type of hydroxyapatite, the old generation with increase grains under 100 nm and the new generation with very fine grains of HA under 20 nm and very aglomerate. The aglomeration with hydroxyapatite are very pronounced.

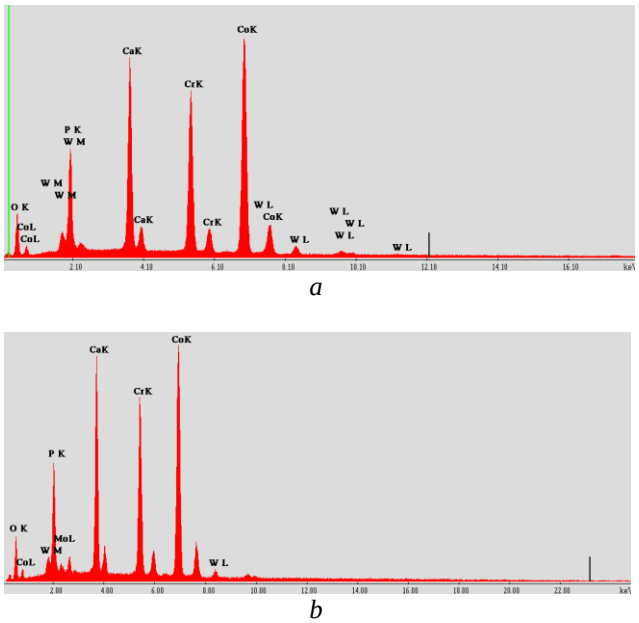

Fig. 15. EDS analyses of Co-Cr sintered compact doped with 15%HA: a) initially; b) after immersion in SBF for 7 days

Growth the quantity of very fine grains was evidenced. EDS and XRD analyses determine the quantity of hydroxyapatite and the growth concentration of HA after immersion in SBF. In EDS analyse, the bright contrast areas represent the heavy elements with high atomic number, like W, Cr, Co and Fe and contrast grey areas containing easy elements like Ca.

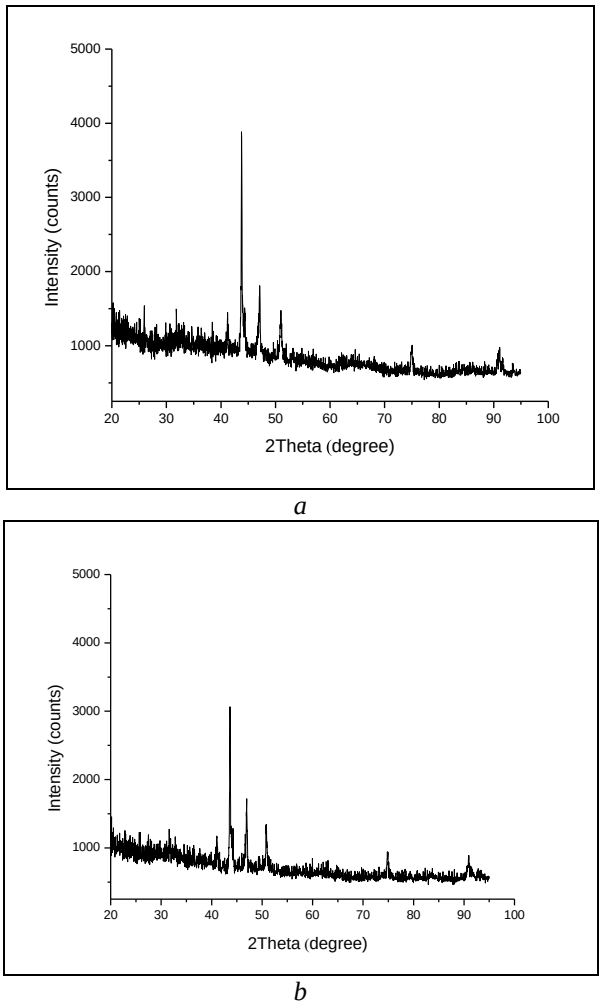

Fig. 16. XRD patterns of Co-Cr sintered compact doped with 15% HA: a) initially; b) after immersion in SBF for 7 days

After immesion in SBF during 7 days, XRD presents the presence of HA peaks and remarck modifications concerning the chemical composition of the sintered compact of Co-Cr with 15%HA.

XRD analyse presents the existance of $Ca_5(PO_4)_3(OH)$, calcium phosphate hydroxide with hexagonal crystal system, P63/m space group, 176 space group number.

XRD analysis determine the growth of HA peaks, after imerssion in SBF and present modifications concerning the chemical composition of the sintered compact of Co-Cr with 15%HA. The growth pics of calcium phosphate hydroxide $Ca_5(PO_4)_3(OH)$ are observed by XRD analysis.

3.5 Co-Cr compact sintered doped with 20%HA

Concerning Co-Cr sintered compact with 20% HA remark large amount of grey grain of HA.

In the Fig. 17 (x1000) the homogeneity mixing Co-Cr with 20% HA is remarked. Figure 18 show EDS results and the homogeneity of elements in the sintered compact were evidenced. The peaks of Ca, P increased in EDS after immersion in SBF. Hydroxyapatite has irregular and elongated grains with nanometer size. In the Fig. 19 XRD pattern revealed the increase of HA.

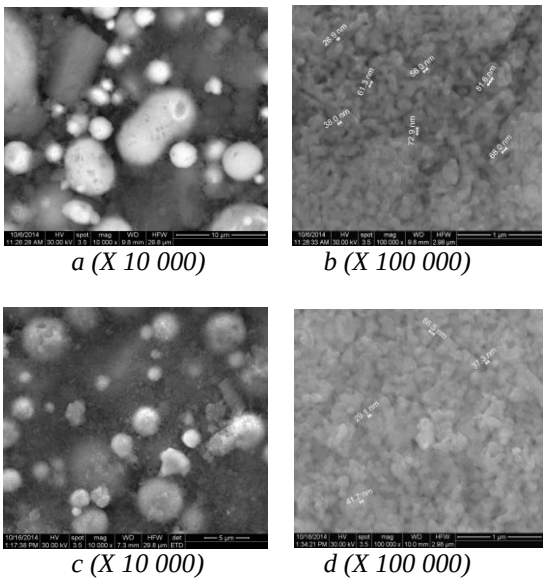

Fig. 17. SEM images of Co-Cr sintered compact doped with 20%HA: a,b) initially and c,d) after immersion in SBF for 7 days

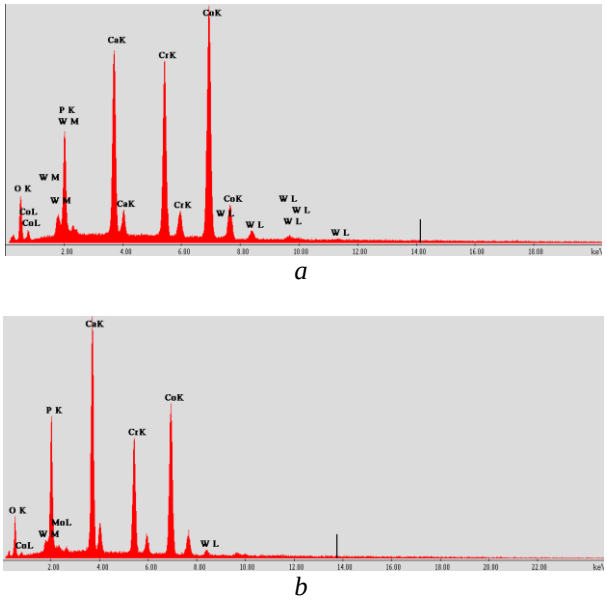

Fig. 18. EDS analyses of Co-Cr sintered compact doped with 20%HA: a) initially and b) after immersion in SBF for 7 days

After immersion for 7 days in SBF, for the Co-Cr sintered compact doped with 20%HA can be seen a total covering with hydroxyapatite. The Co-Cr grains are covered with a generous layer of hydroxyapatite. It is remarked the majority presence of HA with very fine grains. The aspect of sintered compact with 20%HA show a majority of the new generation of HA obtained after imerssion in SBF, with very fine grains of 29 nm size. The aglomeration with hydroxyapatite is very pronounced. EDS and XRD analyses determine the quantity of hydroxyapatite and the growth concentration of HA after immersion in SBF. The interface diffusion between hydroxyapatite and Co-Cr matrix is put in evidence by EDS spectrum. EDS analyse shows bright contrast areas (heavy elements with high atomic number) containing W, Cr, Co and Fe and contrast grey areas containing Ca.

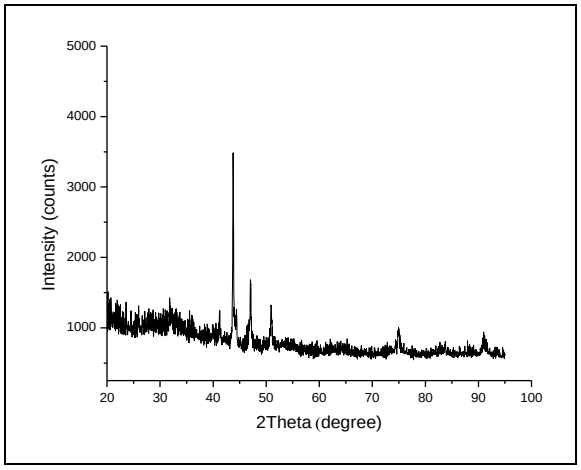

a

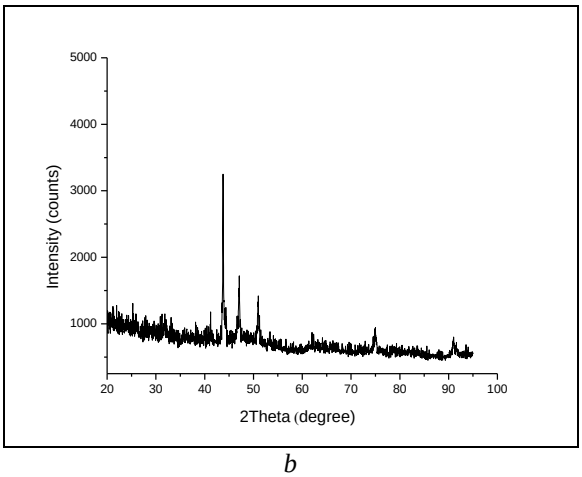

b

Fig. 19. XRD patterns of Co-Cr sintered compact doped with 20% HA: a) initially; b) after immersion in SBF for 7 days

After imerssion in SBF, on the sintered compact Co-Cr with 20%HA, XRD analyses show the growth of HA peaks (calcium phosphate hydroxide) $Ca_5(PO_4)_3(OH)$ and present modifications concerning the chemical composition.

The Co-Cr sintered compact with 5% HA presents smalls HA peaks observed in EDS. The presence of HA in compact was well evidenced by SEM images.

After immersion of Co-Cr sintered compact with 5% HA in SBF a growth of HA on the surface was observed.

For the Co-Cr compact sintered doped with 10% HA the presence of two generations of hydroxyapatite grains was presented in SEM images. Different areas with hydroxyapatite aglomerations can be observe by SEM because of the new hydroxyapatite grains obtains after imersion in SBF.

In the case of the Co-Cr sintered compact with 15% HA was observed the presence of two generations of hydroxyapatite. Old generation presents an increased grains of ~100 nm and the new generation has very fine and aglomerate grains of HA under 20 nm. The growth of hydroxyapatite HA after immersion in SBF was determined by EDS and XRD. The compact sintered Co-Cr with 20% HA has the majority presence of HA with very fine grains of HA.

The majority generation of HA is the new hydroxyapatite with very fine grains, 29 nm size, obtain after imerssion in SBF, results after SEM, EDS and XRD analysis. The aglomeration with hydroxyapatite are very pronounced.

4. Conclusions

In this paper, sintered compacts based on Co-Cr doped with hydroxyapatite (5%, 10%, 15%, 20% by mass) were obtained in order to use them for implants. Doping with HA had a beneficial effect in increasing the bioactivity. Treatment of compacts sintered at 700°C changed the hydroxyapatite morphology from needle shape in the form of rods. SEM results show a high homogeneity of hydroxyapatite and Co-Cr powder in all compacts regardless of the amount used for doping.

Like in the case of the sintered compacts of Ti6Al4V doped with hydroxyapatite to 700^{o}C, for Co-Cr sintered compacts doped with HA can remark the growth of hydroxyapatite concentrations after immersion in SBF, determined by XRD, EDS and SEM analysis, what means a better osteointegration in the human tissues.

XRD and EDS analysis shows the increasing of bioactivity on the compacts by growth of hydroxyapatite peaks and concentrations. The increasing quantity of hydroxyapatite permits a better adheration of implants to the bone tissues.

After placing all compacts in SBF show the growth of hydroxyapatite on the surface. Compacts sintered Co-Cr-doped 15% HA and 20% HA shows the largest increase of HA peaks, relative to the Co-Cr sintered compacts doped with 5% HA and 10% HA.

Concerning the mechanical strength, the optimal compacts that may be used for dental implants are Co-Cr sintered compacts doped with 10% HA and 15% HA.

Acknowledgement

This work is supported by the Sectorial Operational Programme Human Resources Development (SOP HRD), financed from the European Social Fund and the Romanian Government, under the contract number POSDRU/159/1.5/S/138963 – PERFORM.

References

[1] N. Patel, S.M. Best, I.R. Gibson, K.A. Bonfield, Bioceramics, **13**, 192 (2001).
[2] E. Ozgur, Bioceramics, J. Am. Ceram. Soc. **83(**7), 1581 (2000).
[3] D.R. Buddy, S. Hoffman, F. Schoen, J. Lemons, Biomaterials Science, An introduction to materials in medicine, Academic Press (1996).
[4] K.G. Sangamesh, T. Gato, D. Meng, Natural and synthetic biomedical polymers, Elsevier SUA, (2013).
[5] F.H. Silver, L. David, Biomaterials science and biocompatibility. Springer Verlag, (1999).
[6] B.P. Joon, J.D. Bronzi, Biomaterials. Principles and Applications, CRC Press (1999),
[7] W. Schatt, K.P. Wieters, Powder Metallurgy. Processing and materials EPMA, (1997).
[8] I. Vida-Simiti, Technological properties in powders metallurgy - Editura Enciclopedică, Bucureşti (1999).
[9] A.F. von Recum, Handbook of Biomaterials-Evaluation – second edition, (1999).
[10] H.V. Buf, G. Buşilă, Third Conference in Powder metallurgy, Cluj-Napoca (RO), 1998, p.169-174.
[11] D.I. Băilă, Theoretical and experimental researches concerning the assimilation of new biocompatible materials manufacturing by Rapid Prototyping Technologies (Cercetari teoretice şi experimentale privind asimilarea de noi materiale prelucrabile prin tehnologiile Rapid Prototyping)- Doctoral Thesis, (2009).
[12] D.I. Băilă, L.V. Lazăr, Advanced Materials Research Journal; **680**, 59 (2013).
[13] D.I. Băilă, ISI Proceedings DAAAM Zadar Croatia, 2013, p.594.
[14] M. Bahraminasab, B. Bin Sahari, Promising Materials in Orthopedic Applications, INTECH; 2013, p.261.
[15] C.L. Chu, C.Y. Chung, P.H. Lin, S.D. Wang, Materials Science and Engineering: A; **366**, 114 (2004).
[16] M. Iijima, B.A. Brantley, W.H. Guo, W. Clark, T. Yuasa, I. Mizoguchi, Dental Materials; **24**, 1454 (2008).
[17] F.L. Nie, S.G. Wang, Y.B. Wang, S.C. Wei, Y.F. Zang, Dental Materials. **27**, 677 (2011).
[18] Y.C. Tang, S. Katsuma, S. Fujimoto, S. Hiromoto, Acta Biomaterialia. **2**, 709 (2006).
[19] T. Hryniewicz, K. Rokosz, M. Filippi, Materials Journal. **2**, 129 (2009).
[20] J.A. Hunt, J.T. Callaghan, C.J. Sutcliffe, R.H. Morgan, B. Halford, R.A. Black, Biomaterials Journal. **26**, 5890 (2005).
[21] J.P. Boutrand, Biocompatibility and performance of medical devices. Woodhead Publishing Series in Biomaterials, (2012).
[22] D.I. Băilă, Applied Mechanics and Materials J. **467**, 192 (2013).
[23] D.I. Băilă, Advanced Materials Research J. **856**, 164 (2013).
[24] http://www.phenix-systems.com/en/materials
[25] P. Berce, M. Ancau, N. Balc, C. Caizer, S. Comsa, H. Chezan, Rapid Prototyping Manufacturing, Tehnical Publishing, Bucharest, 2000, p 20-30.
[26] W. Schatt, K.P. Wieters, Powder Metallurgy. Processing and materials EPMA, (1997).
[27] P.J. Da Silva Bartolo, A.C. Soares de Lemos, A.M. Henriques Pereira, High Value Manufacturing: Advanced Research in Virtual and Rapid Prototyping, CRC Press, (2013).
[28] R. Narayan, Rapid Prototyping of biomaterials: Principles and Applications, Woodhead Publishing Series in Biomaterials, (2013).
[29] J.C. Ferreira, Rapid Prototyping and 3D Scanning in the Portuguese foundry industry, Proceedings of the 6th European Conference on Rapid Prototyping and Manufacturing, Notthingham(UK), 1997, p 157-166.
[30] P. Greenbaum, S. Khan, Direct Investement Casting of RP Parts, Proceeding of the 5th European Conference on Rapid Prototyping and Manufacturing, Nottingham (UK), 1993, p.77-94.
[31] K. Nutt, The SLS Selective Laser Sintering Process, Proceedings of the 1st European Conference on Rapid Prototyping, Nottingham (UK), 1992, p.51-58.
[32] M. Warner, Time-Compression Technologies; **6**, 45 (1998)
[33] C. Mirestean, P. Berce, S. Simion, J. Optoelectron. Adv. Mater. **12(**9), 1899 (2010).
[34] I. Gligor, I. Marcu, M. Todea, L. Cont, V. Candea, C. Popa, J. Optoelectron. Adv. Mater., **13**(7), 882 (2011).

Corresponding author: baila_d@yahoo.com